RNAi mediated silencing of Nanog expression suppresses the growth of human colorectal cancer stem cells

Chen Zhang
Minjiang University
Yuanyuan Zhao
Jilin University
Yongjing Yang
Cancer Hospital of Jilin Pronvince
Chunlian Zhong
Minjiang University
Tianju Ji
Jilin University
Jinyue Duan
Jilin University
Yi Wang (room1129@163.com)
Jilin University https://orcid.org/0000-0003-4021-1067

Research article

Keywords: Colorectal cancer, Cancer stem cells, Nanog, Proliferation, Apoptosis, Tumor growth

Posted Date: August 13th, 2020

DOI: https://doi.org/10.21203/rs.3.rs-22167/v2

Version of Record: A version of this preprint was published at Biochemical and Biophysical Research Communications on January 1st, 2021. See the published version at https://doi.org/10.1016/j.bbrc.2020.11.101.

Abstract

Background: Colorectal cancer (CRC) is the third most common cancer in the world known for its poor recurrence-free prognosis. Previous studies have shown that it is closely linked with cancer stem cells (CSCs), which have self-renewal potential and the capacity to differentiate into diverse populations. Nanog is an important transcription factor that functions to maintain the self-renewal and proliferation of embryonic stem cells; however, many recent studies have shown that Nanog is also highly expressed in many cancer stem cells.

Methods: To investigate whether Nanog plays a crucial role in maintaining the stemness of colorectal CSCs (CCSCs), RNA interference was used to downregulate Nanog expression in the CRC stem cell line, EpCAM + CD44 + HCT-116. We examined the anti-tumor function of Nanog in vitro and in vivo, using small interfering RNA.

Results: Our results revealed that the Nanog mRNA expression level in CCSCs was higher than that in HCT-116 cells. We found that the depletion of Nanog inhibited proliferation and promoted apoptosis in EpCAM + CD44 + HCT-116 cells. In addition, the invasive ability of EpCAM + CD44 + HCT-116 cells was markedly restricted when Nanog was silenced by small interfering RNA. Furthermore, we found that the silencing of Nanog decreased tumor size and weight and improved the survival rate of tumor-bearing mice.

Conclusions: In conclusion, these findings collectively demonstrate that Nanog, which is highly expressed in CRC stem cells, is a key factor in the development of tumor growth, and it may serve as a potential marker of prognosis and a novel and effective therapeutic target for the treatment of CRC.

Background

Colorectal cancer (CRC) is one of the most common malignant neoplasms with poor prognosis and high frequency of recurrence[1], accounting for 600,000 mortalities per year worldwide. Tumor recurrence and metastasis to distant organs are the main factors for the high mortality and low survival rates[2]. Although the incidence of CRC has decreased, current treatments have serious side effects, with a recurrence rate of more than 50%, mainly due to resistance to conventional chemotherapy drugs[3, 4].

Recent studies have shown that cancer stem cells (CSCs), which are present in many tumors, are a subset of cancer cells with the ability to self-renew. CSCs are primarily implicated in tumor initiation, progression, metastasis, and relapse after therapy [5-8]. The ineffectiveness of current cancer treatments may be the result of increased resistance of CSCs [9]. Thus, it is vital to improve the current therapeutic strategies for CRC and find novel treatments to eradicate cancer stem cells.

Nanog is a unique homeobox transcription factor required to maintain the self-renewal and pluripotency of embryonic stem cells (ESCs). Recently, emerging evidences have demonstrated that Nanog is expressed in a variety of cancer cell lines and tissues, and is associated with aggressive tumors [10, 11].

A number of studies have revealed that the Nanog is a biomarker of CSCs, regulating cancer progression [12], as well as playing an important role in proliferation, apoptosis, differentiation, and stress response in CSCs in many cancers such as cervical, breast, and bladder cancers [12-16]. Several lines of evidence have suggested that the expression of *Nanog* is closely related to tumorigenesis, tumor metastasis, and distant recurrence after treatment [17]. Nanog plays key role in maintaining CSC status and evasive resistance to conventional chemotherapy in bladder cancer stem cells and lung cancer stem cells [18, 19]. However, the potential role of Nanog in CSC in CRC remains to be elucidated.

In our previous study, we found that Nanog mRNA expression in colon cancer stem cells (CCSCs) was higher than that in the total CRC cells. In the present study, we used RNA interference technology to silence Nanog mRNA and to examine the effect of Nanog on CCSCs. The results showed that silencing of Nanog suppressed proliferation, invasion, and tumorigenesis, as well as induced apoptosis of CCSCs, thus laying a foundation for further studies on the biological characteristics of CCSCs. Our findings also suggest that Nanog could be a novel therapeutic target in CRC.

Methods

Cell lines and cell culture

Before magnetic sorting, human CRC (HCT)-116 cells (Cell Bank, Chinese Academy of Sciences, Shanghai, China) were cultured in adhering form (2D culture) in RPMI 1640 medium supplemented with 10% fetal bovine serum (FBS). After magnetic sorting, $EpCAM^{+}CD44^{+}$HCT-116 cells (CCSCs) were cultured in Dulbecco's modified Eagle's medium with Ham's F12 (DMEM/F12) containing 2% B27, 20 ng/ml basic fibroblast growth factor (bFGF), and 20 ng/ml epidermal growth factor (EGF) as we previously described[6] to promote 3D forms (colon spheres). The cells were cultured in an incubator at 37°C containing 5% CO_2.

Animals

A total of 35 6-week-old female athymic BALB/c nude mice (20±2 g) were purchased from Beijing HFK Bioscience Co., Ltd. and housed in the Laboratory Animal Center at Jilin University. All animals bred in specific pathogen-free conditions, with 25±2℃ temperature, 55±5% humidity and a 12-h light/ dark cycle as the same conditions previously described [20]. Animals had ad libitum access to water and mouse chow diet. An acclimation period of at least 1 week was implemented for all mice prior to use in experiments. All the procedures were approved by Animal Care Committee of Jilin University (No. 2019-0046) and performed according to the Jilin University Guidelines for Animal Research.

Reagents and antibodies

The RPMI 1640 and DMEM/F12 were bought from Gibco (Grand Island, NY, USA) and the bFGF and EGF were purchased from PEPROTECH (Rocky Hill, NJ, USA). Anti-human CD44-biotin and anti-human epithelial cell adhesion molecule (EpCAM) for magnetic-activated cell sorting (MACS), were both purchased from eBioscience (San Diego, CA, USA). Phycoerythrin (PE)-anti-human CD44 and fluorescein isothiocyanate (FITC)-anti-EpCAM (eBioscience) were used for flow cytometric analysis. Mouse anti-Nanog and anti-GAPDH antibodies (Biolegend, San Diego, CA, USA), mouse anti-MMP-9, mouse anti-MMP-2, mouse anti-Bax, mouse anti-Bcl-2, rabbit anti-cleaved caspase-3, rabbit anti-TIMP-1 were purchased from Abcam (Cambrige, UK) using for western blotting.

Magnetic activated cell sorting (MACS)

As we previously described, the experiment of MACS was performed using a CELLection™ Biotin Binder kit following the manufacturer's instructions [6].In brief, HCT-116 cells were collected and incubated with anti-human EpCAM-biotin at 4°C for 10 min. Subsequently, the cells were labeled with dynabeads (500 μl) for 20 min at 4°C, and a magnet was used to obtain the labeled cells ($EpCAM^+$ cells). $EpCAM^+$ cells were then incubated in releasing buffer (100 μg/mL Dnase I) for 15 min at room temperature (RT) and collected. $EpCAM^+$ cells were incubated with anti-human CD44-biotin for 10 min, and subsequently with dynabeads (50 μl) for 20 min. Target cells ($EPCAM^+CD44^+$ CCSCs) were separated using a magnet after adding releasing buffer (100 μg/mL Dnase I) into the cells and incubating for 15 min at RT. $EpCAM^+/CD44^+$ CCSCs were freshly prepared for use.

Silencing by siRNA transfection

To inhibit Nanog expression in the EpCAM+ CD44+ HCT-116 cells (CCSCs), silencing by small interfering RNAs (siRNAs) was performed using riboFECT^{TM} CP Transfection Kit (Ribobio, Guangzhou, China) according to the manufacturer's instructions. Nanog siRNA and its negative siRNA control were designed and synthesized by Riobobio (Guangzhou, China). Nanog siRNA sequence is 5'-AACTATCCATCCTTGCAAA-3'. The CCSCs were first cultured in 6-well plates (10^6 cells/well) in DMEM/F12 medium for 48 h, and then transfected with 20 μM Nanog siRNA or negative siRNA control. Cells that had not been transfected served as controls. After transfection for 48 h, the cells were cultured for further evaluation.

Flow cytometry

The cells (10^6/tube) were washed twice with phosphate-buffered saline (PBS) and incubated with PE-anti-human CD44 and FITC-anti-human EpCAM (appropriate dilution per antibody) at 4°C for 20 min.

Subsequently, the cells were washed with PBS twice. The labeled cells were analyzed using a flow cytometer (Beckman Coulter, Inc., Brea, CA, USA).

Serum-induced differentiation

To induce differentiation, CCSCs were cultured in DMEM/F12 medium supplemented with 10% FBS for 3 days. The results were observed using an inverted microscope (Olympus IX71, Tokyo, Japan).

Single-cell colony formation

$EpCAM^+$ $CD44^+$HCT-116 cells were seeded in DMEM/F12 medium at a density of 200 cells per well on 6-well plates and cultured at 37°C for 3 weeks. The medium was replaced every 2 to 3 days. Plates were photographed with an optical inverted microscope (Olympus IX71, Tokyo, Japan).

Quantitative real-time polymerase chain reaction (qRT-PCR)

Total cellular RNA was extracted using TRIzol reagent (Invitrogen, USA); reverse transcription was performed from 1 μg of the total RNA using PrimeScript RT Master Mix (TaKaRa, Dalian, China), according to the manufacturer's instructions. qRT-PCR was performed with TransStart Top Green qPCR SuperMix (TransGen, Beijing, China) using a real-time PCR system (PikoReal 96, ThermoFisher Scientific, USA) with the following program: 94°C for 30 sec, followed by 40 cycles of amplification (94°C for 5 sec, 60°C for 15 sec, and 72°C for 1 sec). The primer sequences (GeneCreate, Wuhan, China) used for quantitative real-time PCR are shown in Table 1. GAPDH was used as an endogenous control. The relative expression levels of mRNA transcripts were analyzed by the $2^{-\Delta\Delta Ct}$ method. All the experiments were performed in triplicate.

Western blot analysis

The CCSCs transfected with Nanog siRNA or negative siRNA control were harvested 48 h after transfection. For western blot analysis, cells were lysed in radioimmunoprecipitation assay (RIPA) buffer containing a protease inhibitor (DINGGUO, Beijing, China). After quantification of protein concentrations using a BCA protein assay kit (Beyotime, Nanjing, Jiangsu, China), equivalent quantities of protein (30 μg/well) were separated by 12% sodium dodecyl sulfate-polyacrylamide gel electrophoresis (SDS-PAGE) and transferred to polyvinylidene fluoride (PVDF) membranes. The membranes were incubated in blocking solution (5% non-fat milk/TBST), and then incubated with the following primary antibodies overnight at 4°C: mouse anti-Nanog (1:1000), mouse anti-MMP-9 (1:500), mouse anti-MMP-2 (1:500),

mouse anti-Bax (1:500), mouse anti-Bcl-2 (1:500), rabbit anti-cleaved caspase-3 (1:500), rabbit anti-TIMP-1 (1:500) and mouse anti-GAPDH (1:2000). After being washed three times with TBST, the membranes were incubated with horseradish peroxidase (HRP)-conjugated secondary antibody for 1 h at RT. Then, the membranes were washed again three times with TBST. The protein bands were detected using enhanced chemiluminescence detection kit (ECL; Beyotime, Nanjing, Jiangsu, China) on ChemiDoc XPS system (Bio-Rad, USA), and GAPDH was used as the loading control. Protein expression was quantified using Image Lab 5.2.1 (Bio-Rad) and normalized to GAPDH.

MTS cell proliferation assay

Cell proliferation was assessed using CellTiter 96 Aqueous assay kit (Promega; Madison, WI, USA). The CCSCs transfected with Nanog siRNA or negative siRNA control were plated at a density of 10^4 cells/well into 96-well plates (100 µl medium/well). After 48 h, 40 µl of 3-(4,5-dimethylthiazol-2-yl)-5-(3-C-arboxymethoxyphenyl)-2-(sulfophenyl)-2H-tetrazolium solution (MTS) was added to each well according to the manufacturer's instructions, followed by incubation of the plates at 37°C, 5% CO_2 for 2 h, and the absorbance was measured at 490 nm using a microplate reader (Scientific Multiskan GO, Thermo, MA, USA). All experiments were performed in triplicate and repeated three times.

Annexin V analysis

Annexin V analysis was performed using the -Annexin V-FITC kit (KeyGEN, Nanjing, Jiangsu, China) according to the manufacturer's instructions. Briefly, after 48 hours' transfection of CCSC with Nanog siRNA or negative siRNA control, they were harvested and washed twice with PBS and then re-suspended in binding buffer at a density of 1×10^6 cells/ml. Subsequently, Annexin V-FITC (5µl) and propidium iodide (PI) (5µl) were added to the cells (500 µl). After being incubated for 15 min in the dark at RT, the cells were analyzed using a flow cytometer (BD Biosciences, USA). Annexin V^-/PI^- cells present cell survival, Annexin V^+/PI^- cells were shown cells in early apoptosis, and Annexin V^+/PI^+ cells were in late apoptosis or necrotic. The experiments were repeated independently three times.

JC-1 assay

Alterations in mitochondrial membrane potential were measured by flow cytometry using the JC-1 kit (KeyGEN, Nanjing, Jiangsu, China) according to the manufacturer's instructions. Briefly, after 48 hours' transfection of CCSC with Nanog siRNA or negative siRNA control, the cells were harvested and washed twice with PBS and re-suspended in 500 µl incubation buffer containing the JC-1 dye (1 µl) at a density of 1×10^6 cells/ml. After being incubated for 15 min at 37°C, 5% CO_2, the cells were collected and washed

twice with the incubation buffer. Subsequently, cells were re-suspended in 500 μl incubation buffer and analyzed using a flow cytometer (BD Biosciences, USA).

Transwell invasion assay

The invasion assays were performed using 6.5-mm diameter Transwell plates (8 μm pore size, Corning, Steuben County, NY, USA) coated with a thin layer of Matrigel (BD Biosciences, San Diego, CA, USA), through which invading cells could migrate and eventually attach to the bottom of the polycarbonate layer. The CCSCs were resuspended in serum free DMEM/F12 at a concentration of 1×10^6/ml. The upper chamber was loaded with 100 μl of cell suspension and the lower chamber was loaded with 500 μl of DMEM/F12 medium supplemented with 10% FBS as the chemoattractant. After incubation for 24 h at 37°C and 5% CO_2, non-invading cells in the upper chamber were removed with a PBS-soaked cotton swab and the cells that had invaded the membranes were stained with 0.5% crystal violet and counted under a light microscope. Each assay was replicated 3 times. The invaded cells were counted under the microscope in five random fields in each chamber. The assay was performed in triplicate.

In vivo tumor xenograft assay

To generate tumor xenografts, $EpCAM^+CD44^+$HCT-116 cells (5×10^5) were injected subcutaneously into the right flank of each mouse. When the mice attained a tumor volume of 40-60 mm^3, they were randomly divided into 3 groups (n = 10) and treated with Nanog siRNA, mock, or negative siRNA control. Nanog siRNA or negative siRNA control was injected intratumorally twice a week for 3 weeks. The tumor size was measured every other day using a vernier caliper and calculated as $(a\times b^2)/2$, where a is the tumor length and b the width. At the end of the experiment, mice were euthanized by carbon dioxide asphyxiation for approximately 6 min (air displacement rate: 20%/min; carbon dioxide flow rate: 1.7 L/min; the mortality was ensured by cervical dislocation) and tumors were excised and weighed.

Statistical analysis

All data are presented as the mean ± standard deviation (SD) of at least three repeat experiments. Student's t-test and one-way ANOVA analysis were used to analyze the variances between groups. The log-rank test was used to compare the survival rates in different groups. Significant differences were considered when P values were less than 0.05.

Results

Screening and identification of CCSCs from HCT-116 CRC cell lines

EpCAM and CD44 have been previously identified as surface markers for CCSCs and used for isolating CCSCs from CRC cells [21, 22]. In our study, the proportion of the $EpCAM^+CD44^+$ subpopulation of HCT-116 cells isolated by MACS accounted for < 2.00%, and the CCSCs formed spheres after being cultured for 7 days in serum-free medium (**Fig. 1A**). The expressions of EpCAM and CD44 were evaluated by flow cytometry and the percentage of the $EpCAM^+CD44^+$HCT-116 cells in the sorted cells were significantly higher than that in unsorted HCT-116 cells (**Fig. 1B**). Subsequently, CCSC spheres were observed over 21 days by the single-cell colony formation assay (**Fig. 1C**). CCSC spheroid cells became re-adherent and differentiated after serum was added to the medium (**Fig. 1D**).

High expression level of Nanog in CCSCs, and siRNA-mediated knockdown of Nanog

To address whether Nanog can serve as a novel therapeutic target for CRC, the relative mRNAs expression of Nanog is detected in colon cancer cell lines (HCT-116, SW480 and LoVo), the results suggested that there is higher-expression of Nanog in HCT-116 compared with SW480 or LoVo (**Fig. 2A**). Then the relative mRNAs expression of Nanog, Sox-2, Oct-4, and C-myc as putative stem cell markers, were analyzed by real-time PCR in HCT-116 and $EpCAM^+CD44^+$ HCT-116 cells. $EpCAM^+CD44^+$ HCT-116 cells exhibited significantly higher relative Nanog and Oct-4 mRNAs level (7.03±0.12 and 4.37±0.18,) than HCT-116 cells (1.00±0.066 and 1.00±0.17) in **Figure. 2B**. The protein expression of Nanog was also measured by western blot (Fig. 2C and 2D), the result showed that it was significantly higher expression in $EpCAM^+CD44^+$ HCT-116 cells than HCT-116 cells.

To investigate the function of Nanog in CCSCs, Nanog-specific siRNA was transfected into CCSCs (CCSC-siNanog), and its transfection efficiency was analyzed with a fluorescent microscope (**Fig. 2E**). Subsequently, its ability to downregulate Nanog expression was evaluated by RT-qPCR (**Fig. 2F**) and western blot analysis (**Fig. 2G-H**). There was a significant decrease in Nanog expression of mRNA or protein with Nanog-siRNA transfection (mRNA 0.23±0.070, protein 0.33±0.012) compared with mock (mRNA 1.00±0.0064, protein 1.00±0.0083) or negative control (mRNA 0.99±0.048, protein 0.99±0.0078) siRNA transfection, indicating that silencing of Nanog by the siRNA method was effective.

Down-regulation of Nanog inhibits CCSC proliferation and promotes apoptosis

To investigate the effect of Nanog on self-renewal of CCSCs, the MTS cell proliferation assay was performed. Proliferation ratio of CCSC-siNanog group (54.71±8.01 %) was significantly inhibited compared with that of mock (100.00±3.12 %) or negative control groups (96.73±5.72 %) in **Figure. 3A**.

To further examine the effects of Nanog on CCSCs apoptosis, Annexin V and JC-1 assays were performed after Nanog siRNA transfection. The Annexin V/PI assay revealed that compared with Mock (4.16%) or NC siRNA (10.02%) groups, Nanog-siRNA (68.47%) transfection significantly increased the

ratio of Annexin V-positive cells (**Fig. 3C and D**), at the meanwhile, the results of JC-1 staining assay indicated that the percentage of cells undergoing a loss of mitochondrial membrane potential increased significantly following Nanog siRNA (32.31%) transfection compared with Mock (4.94%) or NC siRNA (8.54%) groups (**Fig. 3E and F**).These results suggest that silencing of Nanog promotes CCSC apoptosis. In addition, the expression of B-cell lymphoma 2 (Bcl-2), Bcl-2 associated X protein (Bax), and caspase-3 were evaluated using RT-qPCR and western blot analysis. After treatment with Nanog siRNA for 48 h, the mRNA and protein expression of Bcl-2 (mRNA 0.33±0.027, protein 0.29±0.036) was significantly suppressed while the mRNA and protein expressions of Bax (mRNA 6.07±0.82, protein 5.50±0.041) and cleaved-caspase-3 (mRNA 2.68±0.32, protein 2.07±0.039) were significantly up-regulated (**Fig. 3B, G and H**). Taken together, these results demonstrated that silencing of Nanog inhibited the proliferation of CCSCs and promoted significant apoptosis.

Nanog silencing decreases the invasive ability of CCSCs in vitro

In order to investigate the effect of Nanog on the invasive ability of CRC stem cells, which is often representative of the metastatic potential, the Transwell invasion assay was performed after the silencing of Nanog. Nanog siRNA (62±5) significantly decreased the number of CCSCs that passed through the matrigel compared to those of mock (143±3) or negative siRNA control (140±4) (**Fig. 4A and B**).

Additionally, we analyzed the alterations in the expression of invasion-related genes by RT-qPCR and western blot. After transfection of Nanog siRNA for 48 h, the mRNA and protein expression of matrix metalloproteinases, MMP-2 (mRNA 0.35±0.048, protein0.33±0.038), and MMP-9 (mRNA 0.26±0.068, protein 0.29±0.039), that promote tumor invasion and metastasis, were significantly reduced. However, the expression of tissue inhibitor of metalloproteinases-1 (TIMP-1, mRNA 2.42±0.064, protein 2.32±0.047) was significantly increased in CCSC-siNanog compared with that in mock or negative control CCSCs (**Fig. 4C-E**).

The heat map (summarized the mRNA expression data of Bcl-2, Bax, caspase-3, MMP-2, MMP-9 and TIMP-1) revealed that Nanog silencing enhanced the expression of Bax, caspase-3, and TIMP-1 (**Fig. 5**, in red color), and decreased the expression of Bcl-2, MMP-2, and MMP-9 (**Fig. 5**, in blue color).

Nanog siRNA treatment suppressed tumor growth in vivo and increased mice survival rate

Based on the in vitro studies described above, we further investigated the effect of Nanog siRNA on tumor growth in vivo. A total of 35 of 6-week-old female athymic BALB/c nude mice (20±2 g) were randomly divided into 3 groups (n = 10, note: 5 of mice were excluded because they were no obvious tumors after injected $EpCAM^{+}CD44^{+}$HCT-116 cells for 2 weeks) and treated with Nanog siRNA, mock, or negative siRNA control. After treatment with Nanog siRNA or negative siRNA control (injected intratumorally twice

a week for 3 weeks), we found Nanog siRNA treatment strongly decreased tumor size and weight compared with negative siRNA control or mock treatments (**Fig. 6A and B**). Meanwhile, in comparison with the mock (0/5 mice were alive at day 48, n=5) or control groups (0/5 mice were alive at day 48, n=5), Nanog siRNA treatment (4/5 mice were alive at day 48, n=5) significantly improved the survival rate of tumor-bearing mice (**Fig. 6C**). Taken together, these results demonstrate that Nanog siRNA treatment suppresses colorectal tumor growth in vivo and improves survival, implying that Nanog may serve as a novel therapeutic target for CRC treatment. For survival analysis, mice were sacrificed when tumors measured > 2000 mm^3 or the tumor diameter exceeded 2.0 cm. All of the treatments with mice are according to the protocol of the Animal Care Committee of Jilin University as previously described [20].

Discussion

In recent years, CRC has been ranked as the third leading cause of cancer-related mortalities among malignant tumors worldwide [23]. Advances in the investigation of cancer stem cells have revealed that CSCs have the ability to self-renewal and maintain tumor growth, and therefore play a crucial role in tumorigenesis, development, metastasis, and recurrence [24, 25]. Nanog has been established as an important transcriptional factor required for maintaining self-renewal and pluripotency of embryonic stem cells [23]. Previous studies have shown that Nanog is overexpressed in various types of CSCs [12-14] including CRC stem cells [19]. It is consistent with previous studies [26, 27], the CCSCs in the present study displayed relatively higher expression levels of Nanog compared with that in unsorted HCT-116 cells. M. Zhang et al. illustrated that Nanog siRNA significantly inhibited colony formation, suggesting the indispensable role of Nanog in colon tumor-repopulating cells growth[28]. X. Wang et al. provides cancer-associated mutations of SPOP or the mutation of Nanog at S68Y abrogates the SPOP-mediated Nanog degradation lead to elevated prostate cancer stemness and poor prognosis [29]. Furthermore, emerging evidence has suggested that Nanog plays a vital role during self-renewal of CSCs, and knockdown or silencing of Nanog suppresses CSCs growth and development [30]. These results suggest that Nanog may be associated with tumor initiation, development, and therapeutic resistance. However, the role of Nanog in CRC stem cells has not been investigated.

To understand the functional role of Nanog in CCSCs, we used the RNA interference approach to knockdown Nanog expression in $EpCAM^+CD44^+$HCT-116 cells, and assessed its effect on suppressing growth and promoting apoptosis of CCSCs in vitro. Nanog is a transcription factor involved in the regulation of pluripotency and stemness. The functional paralog of Nanog, NanogP8, differs from Nanog in only three amino acids and exhibits similar reprogramming activity. E. Mikulenkova et al. investigated the intriguing extranuclear localization of Nanog and demonstrated that a substantial pool of Nanog/NanogP8 is localized at the centrosome [31]. NanogP8 is the main regulator of gastric cancer stem cells. It is closely associated with EMT, stemness, and CSC marker as well as Wnt signal pathway. NanogP8 is correlated with cell proliferation, migration, invasion, clonogenic capacity, beta-catenin accumulation in nucleus, and chemoresistance in gastric cancer [32]. B. Liu et al. demonstrated that transgenic overexpression of NanogP8 in the mouse prostate is insufficient to initiate tumorigenesis but

weakly promotes tumor development in the Hi-Myc mouse model [33]. The Nanog siRNA used in this study targets both Nanog and NanogP8. Our results, which revealed that Nanog silencing not only significantly suppressed CCSC proliferation but also markedly induced CCSC apoptosis, ware similar to those of studies reported for pancreatic and breast cancer stem cells [16, 34]. There are two main pathways associated with apoptosis: a pathway mediated by a cell death receptor and that mediated by mitochondrion, both of which lead to the activation of the caspase cascade. Mitochondrial membrane potential is regulated by a complex network of signaling pathways that involve endogenous pro- and anti-apoptotic Bcl-2 family proteins [35]. The results of the Annexin V assays provided evidence that the depletion of Nanog promoted apoptosis of CCSCs, which is in accordance with the results of inhibition of Nanog and aggravation of apoptosis in non-small cell lung cancer [36]. Moreover, the results of JC-1 assays suggested that a loss in mitochondrial transmembrane potential (Δψm) was observed in the Nanog siRNA group compared with that in the mock and negative siRNA control groups. In addition, we analyzed the mRNA levels and protein expression of several apoptosis-related genes since previous studies have shown that resistance to apoptosis is one of the leading causes of tumorigenesis [7, 14, 37]. Caspase-3 is a downstream molecule that is activated by upstream molecules such as caspase-8 or caspase-9, leading to cell apoptosis. Pro-apoptotic Bax promotes the release of pro-apoptotic molecules by forming oligomers in the mitochondrial outer membrane, thus promoting cell apoptosis. Anti-apoptotic Bcl-2 blocks mitochondrial apoptosis by blocking the release and oligomerization of Bax [38]. Thus, Caspase-3 and the Bcl-2 family proteins play an important role in the regulation of apoptosis [39]. Nanog silencing activated cleaved caspase-3 expression, promoted the expression of pro-apoptotic *BAX* gene, and inhibited the expression of anti-apoptotic *Bcl-2* gene. These results indicate that Nanog may play a vital role in the induction of apoptosis in CCSCs via the caspase-3 cascade.

It is well known that the invasive ability of CSCs is crucial for cancer metastasis [40]. Further, high expression levels of matrix metalloproteinases (MMPs), which are identified as potential major regulators of invasion, are associated with tumor progression and metastasis in diverse human cancers [38]. The tissue inhibitors of metalloproteinases (TIMPs), which are inhibitors of MMPs, have been shown to impede tumor progression [41]. In our study, Transwell invasion assay and analyses of mRNA and protein expressions of MMP-2, MMP-9, and TIMP-1, in line with the results of the regulation of MMP-2, 9, and TIMP-1, promote the invasion and metastasis of renal cell carcinoma and MMP-9 (TIMP-1 is its inhibitor) in the degradation of extracellular matrix. This enhances metastasis in breast cancer; thus revealing that Nanog silencing significantly suppressed the invasive potential of CCSCs [42, 43]. Thus, Nanog may play a crucial role in the invasive potential of CSCCs [44]. Consistent with our in vitro results, in vivo results showed that Nanog siRNA significantly suppressed xenograft tumor growth and prolonged mice survival.

Conclusions

In conclusion, our results demonstrated that silencing of Nanog expression suppressed the proliferation, invasion, and tumorigenesis, as well as induced apoptosis of CCSCs in vitro and in vivo, all of which are crucial for cancer development. Furthermore, our findings revealed for the first time the key role of Nanog in tumor growth in CRC. Thus, Nanog-targeted siRNA may provide a possible novel strategy for cancer

stem cell-based targeted therapies in CRC. The exact mechanism by which Nanog silencing exerts its antitumor ability may be worth exploring in future investigations.

Abbreviation

CRC, Colorectal cancer; CSCs, Cancer stem cells; CCSCs, Colorectal CSCs; ESCs, Embryonic stem cells; DMEM/F12, Dulbecco's modified Eagle's medium with Ham’s F12; FBS, Fetal bovine serum; bFGF, Basic fibroblast growth factor; EGF, Epidermal growth factor; EpCAM, Epithelial cell adhesion molecule; MACS, Magnetic-activated cell sorting; PE, Phycoerythrin; FITC, Fluorescein isothiocyanate; RT, Room temperature; siRNA, Small interfering RNA; PBS, Phosphate-buffered saline; qRT-PCR, Quantitative real-time polymerase chain reaction; SDS-PAGE, Sodium dodecyl sulfate-polyacrylamide gel electrophoresis; PVDF, Polyvinylidene fluoride; HRP, Horseradish peroxidase; MTS, 3-(4,5-dimethylthiazol-2-yl)-5-(3-C-arboxymethoxyphenyl)-2-(sulfophenyl)-2H-tetrazolium solution; PI, Propidium iodide; MMPs, Matrix metalloproteinases; TIMPs, Tissue inhibitors of metalloproteinases; Bcl-2, B-cell lymphoma; Bax, Bcl-2 associated X protein.

Declarations

Ethics approval and consent to participate

All experiments and animal care were conducted according to the guidelines established by the Animal Care Committee of Jilin University (Institutional Animal Care and Use Committee of Jilin University School of Pharmaceutical Science, Number of permit: 2019-0046).

Consent for publication

Not applicable.

Availability of data and material

Not applicable.

Competing interests

The author(s) declare that they have no competing interests.

Funding

This work was supported by Jilin Province Science and Technology Support Program (Grant number: 20200404121YY), the Education Department of Jilin Province(Grant number:JJKH20201122KJ), Jilin Province Health Technology Innovation Project (Grant number: 2017J062), National Natural Science Foundation of China (Grant number: 81801849) and Talent Introduction Fund of Minjiang University (Grant number: MJY19011 and MYK19033). The funding body of 2017J062, 81801849, MJY19011 and MYK19033 designed the study, purchased the experimental materials, 20200404121YY collected and analyzed the data; JJKH20201122KJ interpreted the data; 20200404121YY, JJKH20201122KJ and MJY19011 supported in writing the manuscript.

Authors' contributions

C.Z. and Y.Z. conceived the experiment(s), Y.W. conducted the experiment(s), T.J. and J.D. performed the experiments. C.Z., Y.Z., Y.Y. and CL.Z. analyzed the results. C.Z. and Y.Z wrote the manuscript. All authors reviewed the manuscript.

Acknowledgments

Not applicable.

Authors' Information

[1]Department of Regenerative Medicine, School of Pharmaceutical Sciences, Jilin University, Changchun, Jilin 130021, China.

[2]Institute of Oceanography, Minjiang University, Fuzhou, Fujian 350108, China.

[3]Department of Radiation Oncology, Cancer Hospital of Jilin Province, Changchun 130012, China

References

1. Fillon M: **Study aims to improve colorectal cancer screening rates**. *CA Cancer J Clin* 2019, **69**(3):161-163.
2. Dekker E, Rex DK: **Advances in CRC Prevention: Screening and Surveillance**. *Gastroenterology* 2018, **154**(7):1970-1984.
3. Liu ML, Zang F, Zhang SJ: **RBCK1 contributes to chemoresistance and stemness in colorectal cancer (CRC)**. *Biomed Pharmacother* 2019, **118**:109250.

4. Siraj AK, Kumar Parvathareddy S, Pratheeshkumar P, Padmaja Divya S, Ahmed SO, Melosantos R, Begum R, Concepcion R, Al-Sanea N, Ashari LH *et al*: **APC truncating mutations in Middle Eastern Population: Tankyrase inhibitor is an effective strategy to sensitize APC mutant CRC To 5-FU chemotherapy**. *Biomed Pharmacother* 2020, **121**:109572.
5. Dalerba P, Dylla SJ, Park IK, Liu R, Wang X, Cho RW, Hoey T, Gurney A, Huang EH, Simeone DM *et al*: **Phenotypic characterization of human colorectal cancer stem cells**. *Proc Natl Acad Sci U S A* 2007, **104**(24):10158-10163.
6. Zhang C, Tian Y, Song F, Fu C, Han B, Wang Y: **Salinomycin inhibits the growth of colorectal carcinoma by targeting tumor stem cells**. *Oncol Rep* 2015, **34**(5):2469-2476.
7. Zhang C, Gong P, Liu P, Zhou N, Zhou Y, Wang Y: **Thioridazine elicits potent antitumor effects in colorectal cancer stem cells**. *Oncol Rep* 2017, **37**(2):1168-1174.
8. Todaro M, Alea MP, Di Stefano AB, Cammareri P, Vermeulen L, Iovino F, Tripodo C, Russo A, Gulotta G, Medema JP *et al*: **Colon cancer stem cells dictate tumor growth and resist cell death by production of interleukin-4**. *Cell Stem Cell* 2007, **1**(4):389-402.
9. Zhou BBS, Zhang HY, Damelin M, Geles KG, Grindley JC, Dirks PB: **Tumour-initiating cells: challenges and opportunities for anticancer drug discovery**. *Nat Rev Drug Discov* 2009, **8**(10):806-823.
10. Sarkar B, Dosch J, Simeone DM: **Cancer Stem Cells: A New Theory Regarding a Timeless Disease**. *Chem Rev* 2009, **109**(7):3200-3208.
11. Mueller MT, Hermann PC, Witthauer J, Rubio-Viqueira B, Leicht SF, Huber S, Ellwart JW, Mustafa M, Bartenstein P, D'Haese JG *et al*: **Combined Targeted Treatment to Eliminate Tumorigenic Cancer Stem Cells in Human Pancreatic Cancer**. *Gastroenterology* 2009, **137**(3):1102-1113.
12. Jeter CR, Badeaux M, Choy G, Chandra D, Patrawala L, Liu C, Calhoun-Davis T, Zaehres H, Daley GQ, Tang DG: **Functional Evidence that the Self-Renewal Gene NANOG Regulates Human Tumor Development**. *Stem Cells* 2009, **27**(5):993-1005.
13. Lee M, Nam EJ, Kim SW, Kim S, Kim JH, Kim YT: **Prognostic Impact of the Cancer Stem Cell-Related Marker NANOG in Ovarian Serous Carcinoma**. *Int J Gynecol Cancer* 2012, **22**(9):1489-1496.
14. Sun C, Sun L, Jiang K, Gao DM, Kang XN, Wang C, Zhang S, Huang S, Qin X, Li Y *et al*: **NANOG promotes liver cancer cell invasion by inducing epithelial-mesenchymal transition through NODAL/SMAD3 signaling pathway**. *Int J Biochem Cell B* 2013, **45**(6):1099-1108.
15. Jeter CR, Liu B, Liu X, Chen X, Liu C, Calhoun-Davis T, Repass J, Zaehres H, Shen JJ, Tang DG: **NANOG promotes cancer stem cell characteristics and prostate cancer resistance to androgen deprivation**. *Oncogene* 2011, **30**(36):3833-3845.
16. Meng HM, Zheng P, Wang XY, Liu C, Sui HM, Wu SJ, Zhou J, Ding YQ, Li JM: **Overexpression of nanog predicts tumor progression and poor prognosis in colorectal cancer**. *Cancer Biol Ther* 2010, **9**(4):295-302.
17. Yang L, Zhang XD, Zhang MZ, Zhang JH, Sheng YQ, Sun XD, Chen QJ, Wang LX: **Increased Nanog Expression Promotes Tumor Development and Cisplatin Resistance in Human Esophageal Cancer Cells**. *Cell Physiol Biochem* 2012, **30**(4):943-952.

18. Zhang Y, Wang Z, Yu J, Shi JZ, Wang C, Fu WH, Chen ZW, Yang J: **Cancer stem-like cells contribute to cisplatin resistance and progression in bladder cancer**. *Cancer Lett* 2012, **322**(1):70-77.
19. Wang P, Gao QL, Suo ZH, Munthe E, Solberg S, Ma LW, Wang MY, Westerdaal NAC, Kvalheim G, Gaudernack G: **Identification and Characterization of Cells with Cancer Stem Cell Properties in Human Primary Lung Cancer Cell Lines**. *Plos One* 2013, **8**(3).
20. Fu C, Zhou N, Zhao Y, Duan J, Xu H, Wang Y: **Dendritic cells loaded with CD44(+) CT-26 colon cell lysate evoke potent antitumor immune responses**. *Oncol Lett* 2019, **18**(6):5897-5904.
21. Ishiguro T, Sato A, Ohata H, Sakai H, Nakagama H, Okamoto K: **Differential expression of nanog1 and nanogp8 in colon cancer cells**. *Biochem Biophys Res Commun* 2012, **418**(2):199-204.
22. Xu F, Dai CL, Zhang R, Zhao Y, Peng SL, Jia CJ: **Nanog: A Potential Biomarker for Liver Metastasis of Colorectal Cancer**. *Digest Dis Sci* 2012, **57**(9):2340-2346.
23. Chu P, Clanton DJ, Snipas TS, Lee J, Mitchell E, Nguyen ML, Hare E, Peach RJ: **Characterization of a subpopulation of colon cancer cells with stem cell-like properties**. *Int J Cancer* 2009, **124**(6):1312-1321.
24. Zhang N, Yin Y, Xu SJ, Chen WS: **5-Fluorouracil: mechanisms of resistance and reversal strategies**. *Molecules* 2008, **13**(8):1551-1569.
25. Jiang WQ, Fu FF, Li YX, Wang WB, Wang HH, Jiang HP, Teng LS: **Molecular biomarkers of colorectal cancer: prognostic and predictive tools for clinical practice**. *J Zhejiang Univ Sci B* 2012, **13**(9):663-675.
26. Shaheen S, Ahmed M, Lorenzi F, Nateri AS: **Spheroid-Formation (Colonosphere) Assay for in Vitro Assessment and Expansion of Stem Cells in Colon Cancer**. *Stem Cell Rev Rep* 2016, **12**(4):492-499.
27. Pan Q, Meng L, Ye J, Wei X, Shang Y, Tian Y, He Y, Peng Z, Chen L, Chen W *et al*: **Transcriptional repression of miR-200 family members by Nanog in colon cancer cells induces epithelial-mesenchymal transition (EMT)**. *Cancer Lett* 2017, **392**:26-38.
28. Zhang M, Xu C, Wang HZ, Peng YN, Li HO, Zhou YJ, Liu S, Wang F, Liu L, Chang Y *et al*: **Soft fibrin matrix downregulates DAB2IP to promote Nanog-dependent growth of colon tumor-repopulating cells**. *Cell Death Dis* 2019, **10**(3):151.
29. Wang X, Jin J, Wan F, Zhao L, Chu H, Chen C, Liao G, Liu J, Yu Y, Teng H *et al*: **AMPK Promotes SPOP-Mediated NANOG Degradation to Regulate Prostate Cancer Cell Stemness**. *Dev Cell* 2019, **48**(3):345-360 e347.
30. Ibrahim EE, Babaei-Jadidi R, Saadeddin A, Spencer-Dene B, Hossaini S, Abuzinadah M, Li NN, Fadhil W, Ilyas M, Bonnet D *et al*: **Embryonic NANOG Activity Defines Colorectal Cancer Stem Cells and Modulates through AP1-and TCF-dependent Mechanisms**. *Stem Cells* 2012, **30**(10):2076-2087.
31. Mikulenkova E, Neradil J, Vymazal O, Skoda J, Veselska R: **NANOG/NANOGP8 Localizes at the Centrosome and is Spatiotemporally Associated with Centriole Maturation**. *Cells* 2020, **9**(3).
32. Ma X, Wang B, Wang X, Luo Y, Fan W: **NANOGP8 is the key regulator of stemness, EMT, Wnt pathway, chemoresistance, and other malignant phenotypes in gastric cancer cells**. *Plos One* 2018, **13**(4):e0192436.

33. Liu B, Gong S, Li Q, Chen X, Moore J, Suraneni MV, Badeaux MD, Jeter CR, Shen J, Mehmood R *et al*: **Transgenic overexpression of NanogP8 in the mouse prostate is insufficient to initiate tumorigenesis but weakly promotes tumor development in the Hi-Myc mouse model**. *Oncotarget* 2017, **8**(32):52746-52760.
34. Saiki Y, Ishimaru S, Mimori K, Takatsuno Y, Nagahara M, Ishii H, Yamada K, Mori M: **Comprehensive Analysis of the Clinical Significance of Inducing Pluripotent Stemness-Related Gene Expression in Colorectal Cancer Cells**. *Ann Surg Oncol* 2009, **16**(9):2638-2644.
35. Galluzzi L, Brenner C, Morselli E, Touat Z, Kroemer G: **Viral control of mitochondrial apoptosis**. *PLoS Pathog* 2008, **4**(5):e1000018.
36. Chen C, Ju R, Shi J, Chen W, Sun F, Zhu L, Li J, Zhang D, Ye C, Guo L: **Carboxyamidotriazole Synergizes with Sorafenib to Combat Non-Small Cell Lung Cancer through Inhibition of NANOG and Aggravation of Apoptosis**. *J Pharmacol Exp Ther* 2017, **362**(2):219-229.
37. Ambady S, Malcuit C, Kashpur O, Kole D, Holmes WF, Hedblom E, Page RL, Dominko T: **Expression of NANOG and NANOGP8 in a variety of undifferentiated and differentiated human cells**. *Int J Dev Biol* 2010, **54**(11-12):1743-1754.
38. Leibowitz B, Yu J: **Mitochondrial signaling in cell death via the Bcl-2 family**. *Cancer Biol Ther* 2010, **9**(6):417-422.
39. Goodell MA, Brose K, Paradis G, Conner AS, Mulligan RC: **Isolation and functional properties of murine hematopoietic stem cells that are replicating in vivo**. *J Exp Med* 1996, **183**(4):1797-1806.
40. Lee S, Schmitt CA: **Chemotherapy response and resistance**. *Curr Opin Genet Dev* 2003, **13**(1):90-96.
41. Anwar TE, Kleer CG: **Tissue-based identification of stem cells and epithelial-to-mesenchymal transition in breast cancer**. *Hum Pathol* 2013, **44**(8):1457-1464.
42. Lu H, Cao X, Zhang H, Sun G, Fan G, Chen L, Wang S: **Imbalance between MMP-2, 9 and TIMP-1 promote the invasion and metastasis of renal cell carcinoma via SKP2 signaling pathways**. *Tumour Biol* 2014, **35**(10):9807-9813.
43. Zajkowska M, Gacuta E, Kozlowska S, Lubowicka E, Glazewska EK, Chrostek L, Szmitkowski M, Pawlowski P, Zbucka-Kretowska M, Lawicki S: **Diagnostic power of VEGF, MMP-9 and TIMP-1 in patients with breast cancer. A multivariate statistical analysis with ROC curve**. *Adv Med Sci* 2019, **64**(1):1-8.
44. Lee HJ, Noh KH, Lee YH, Song KH, Oh SJ, Kim SY, Kim TW: **NANOG signaling promotes metastatic capability of immunoedited tumor cells**. *Clin Exp Metastasis* 2015, **32**(5):429-439.

Table

Table 1. Primers used for qRT-PCR

Gene	Forward primer 5’→3’	Reverse primer 5’→3’
Nanog	GCCTCACACGGAGACTGTCTCTC	TTCTGGAACCAGGTCTTCACCTG
Caspase-3	CAGAACTGGACTGTGGCATTGAG	GGATGAACCAGGAGCCATCCT
Bax	TAACCAAGGTGCCGGAACTGA	GGGAGGAGTCTCACCCAACCA
Bal-2	GGGGAGGATTGTGGCCTTCTTT	TAATGTGCAGGTGCCGGTTCAG
MMP-2	TCGCCCATCATCAAGTTCCC	TCTGGGGCAGTCCAAAGAAC
MMP-9	GCACCACCACAACATCACCT	ACCACAACTCGTCATCGTCG
Timp-1	TCGTCATCAGGGCCAAGTTC	TCCTGCAGTTTTCCAGCAATG
Oct-4	GCAGCTTGGGCTCGAGAAGGAT	AGCCCAGAGTGGTGACGGAGAC
C-myc	CACCAGCAGCGACTCTGAGGAG	ACTTGACCCTCTTGGCAGCAGG
GAPDH	CATCAGCAATGCCTCCTGCAC	TGAGTCCTTCCACGATACCAAAGTT

Figures

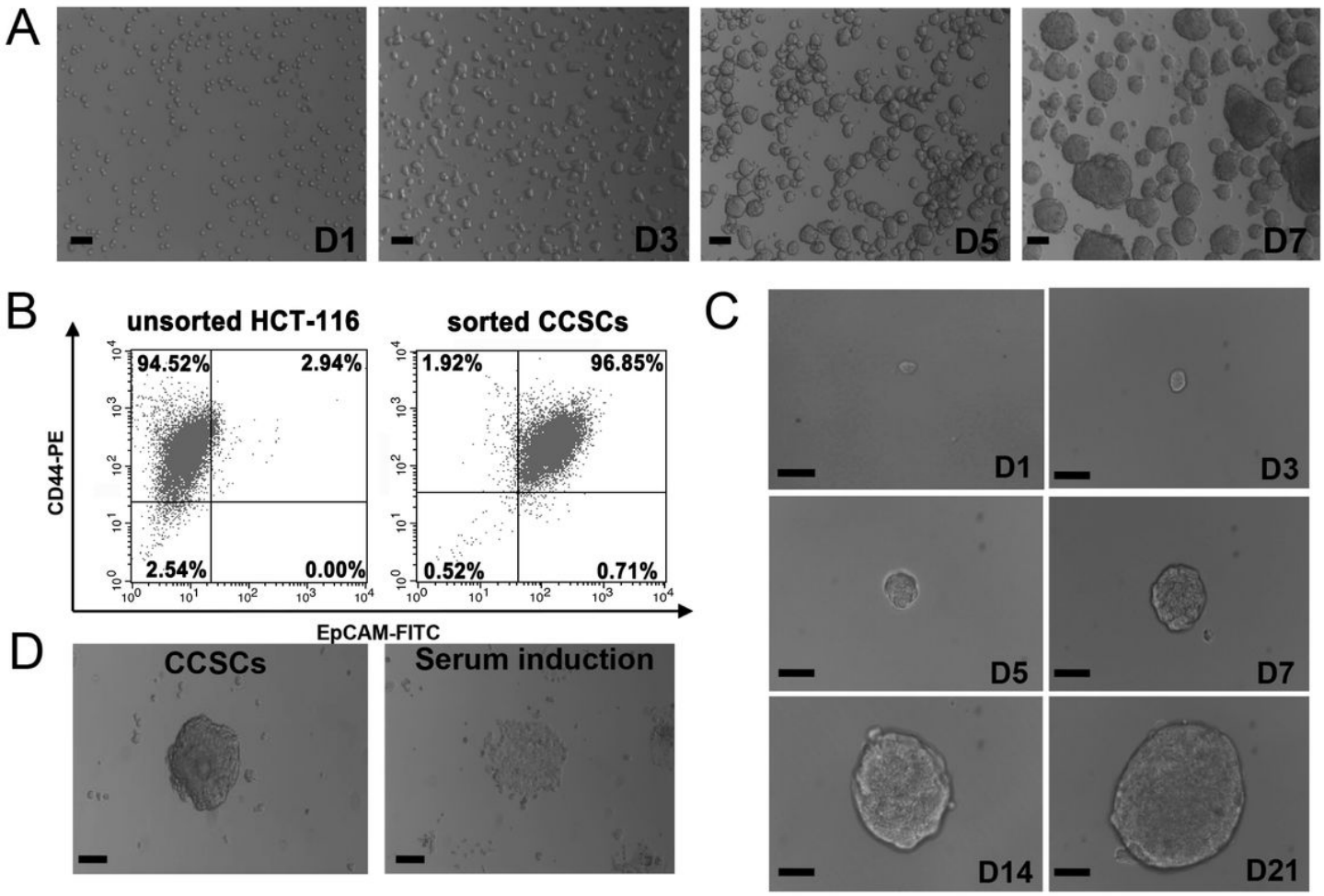

Figure 1

Optical micrographs and identification of sorted EpCAM+CD44+HCT-116 colorectal cancer stem cells (CCSCs). (A) Culture of CCSCs in serum-free DMEM/F12 medium over 7 days. (B) Flow cytometric analysis showing EpCAM and CD44 surface expression in CCSCs and unsorted HCT-116 cells. The majority of CCSCs (96.85%) exhibited EpCAM+CD44+ staining, which was significantly higher than the percentage of unsorted HCT-116 cells (2.94%). (C) Formation of CCSC spheres over 21 days analyzed by single-cell colony formation assay. (D) Serum-induced differentiation of CCSCs into adherent cells. (Scale bar: 200 μm)

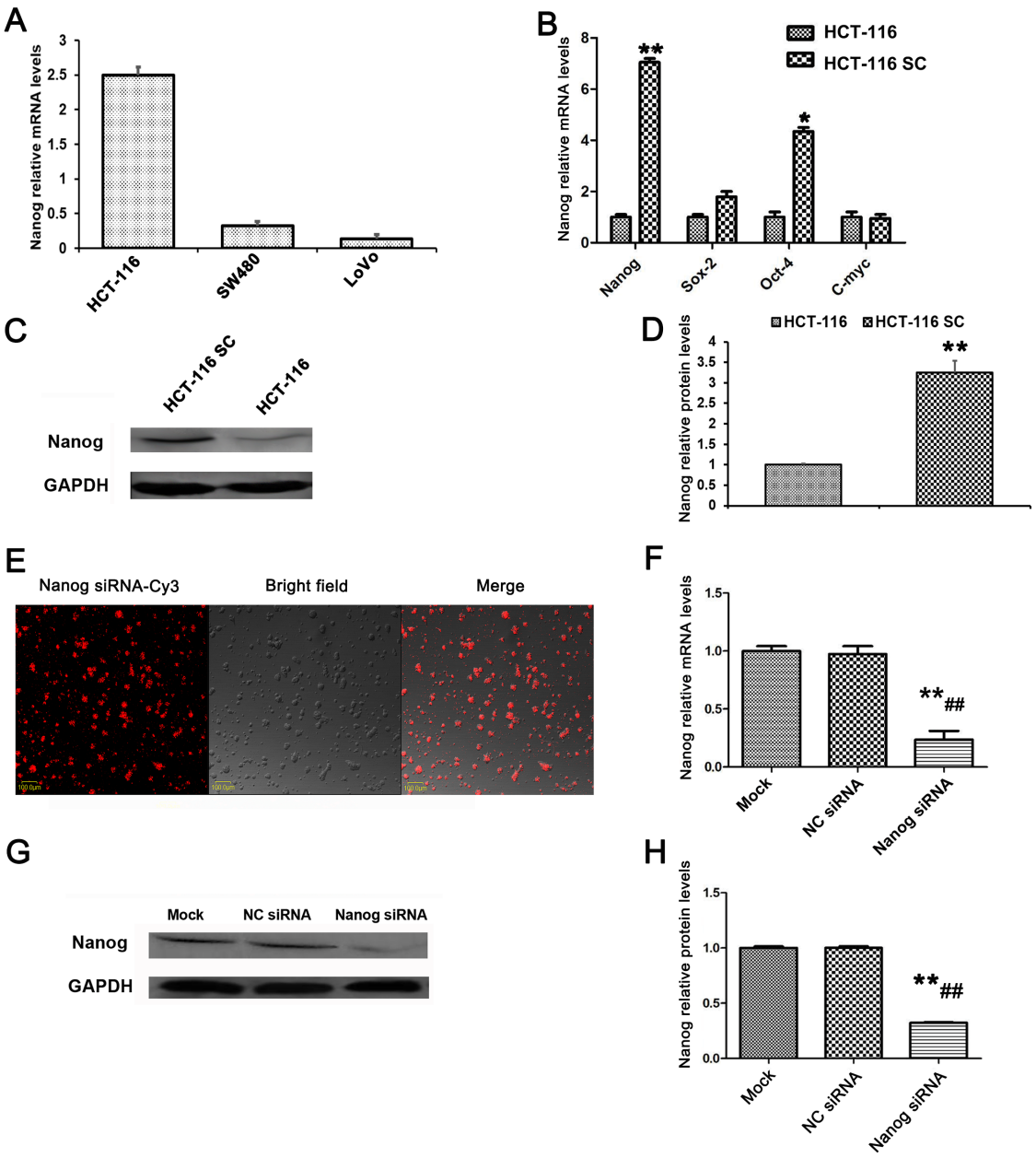

Figure 2

High expression level of Nanog in HCT-116 CSCs and siRNA-mediated down-regulation of Nanog expression. (A) Real-time qPCR analysis showing relative mRNA expression level of Nanog in colon cell lines HCT-116, SW480 and LoVo. (B) Real-time qPCR analysis showing relative mRNA expression level of Nanog in CCSCs compared with that in HCT-116 cells (*P < 0.05, **P < 0.01). (C, D) Western blot analysis showing Nanog protein expression in colon cell lines HCT-116 and EpCAM+CD44+ HCT-116 cells (**P <

0.01). (E) Fluorescent micrographs showing the transfection efficiency of Nanog siRNA. Representative fluorescence images of cy3-linked siRNA (red) are shown. (F) Real-time qPCR analysis showing Nanog mRNA levels in CSCs 48 h after siRNA transfection (**P < 0.01, compared with mock; ##P < 0.01, compared with negative siRNA control). (G, H) Western blot analysis showing Nanog protein expression levels following siRNA transfection of CCSCs. Data represent the means ± SD of three independent experiments (**P < 0.01, compared with mock; ##P < 0.01, compared with negative siRNA control).

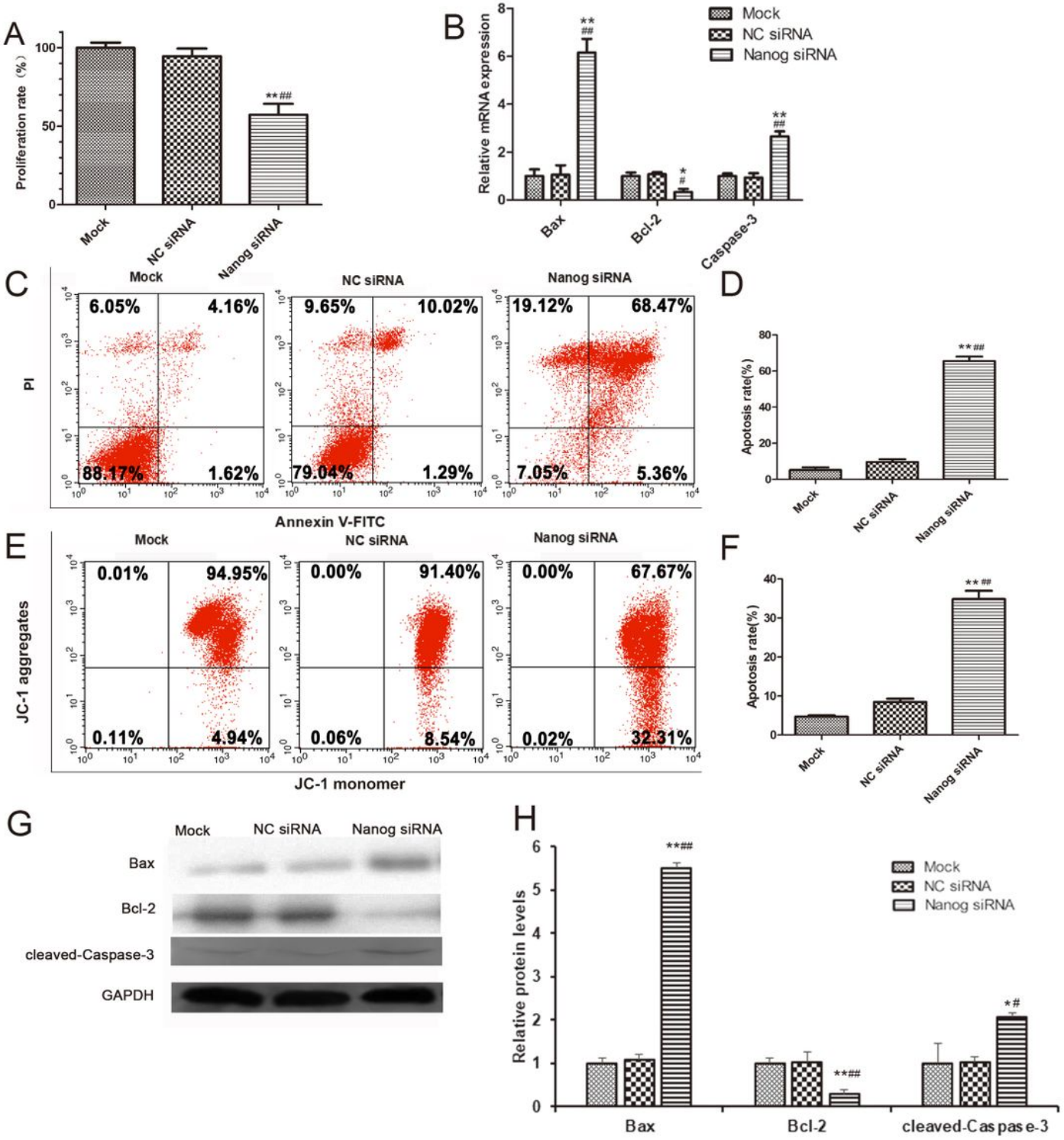

Figure 3

Knockdown of Nanog expression suppresses CCSCs proliferation and induces apoptosis. (A) The MTS cell proliferation assay showing the proliferation potential of CCSCs 48 h after Nanog or control siRNA transfection. (B) Real-time qPCR analysis showing the mRNA levels of Bcl-2, Bax and caspase-3 in CCSCs after transfection with Nanog or control siRNA for 48 h. (C) Flow cytometric analyses of Annexin V/propidium iodide (PI) staining of CCSCs following Nanog or control siRNA transfection for 48 h. Lower-left quadrant, viable cells; upper-right and lower-right quadrants, apoptotic cells; upper-left quadrant, necrotic cells. (D) Annexin V assay results showing the percentage of apoptotic CCSCs after treatment with Nanog or control siRNA. (E) Flow cytometric analysis of JC-1 staining of CCSCs after treatment with Nanog or control siRNA for 48 h. Lower-right quadrant, apoptotic cells. (F) JC-1 assay results showing percentage of apoptotic CCSCs after treatment with Nanog or control siRNA (G, H) Western blot analysis of the protein expression level of Bax, Bcl-2, and cleaved caspase-3 in CCSCs after treatment with Nanog or control siRNA for 48 h. Data represent the means ± SD of three independent experiments. *P < 0.05 and **P < 0.01, compared with mock; #P<0.05 and ##P<0.01, compared with negative siRNA control.

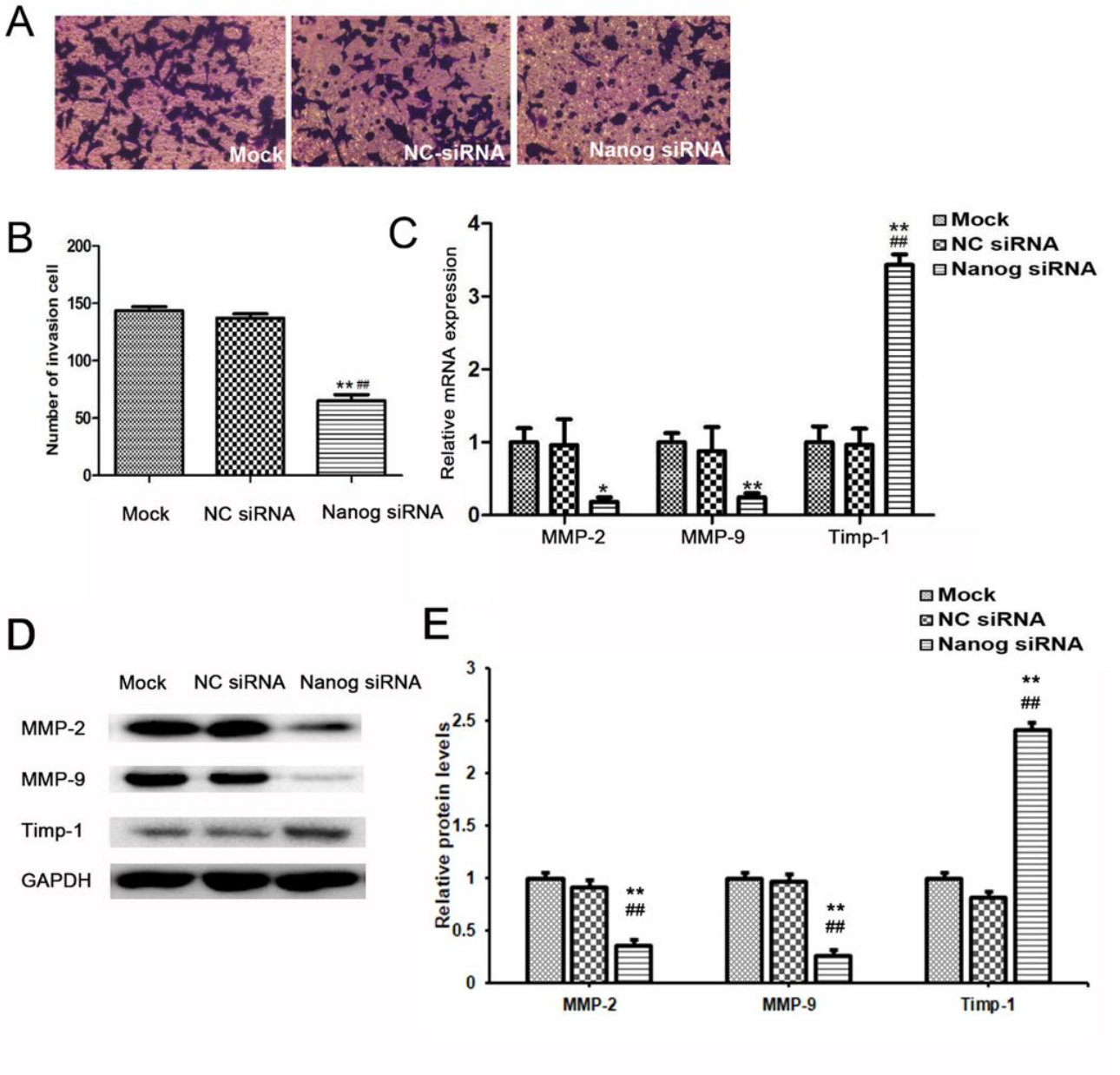

Figure 4

Nanog silencing inhibits the invasive ability of CSCCs in vitro. (A) Representative photographs of cells passed through the matrigel in the Transwell invasion assay. (B) Quantification of the invasion assay indicating the number of invaded CCSCs. (C) Real-time qPCR analysis showing the relative mRNA levels of invasion-related genes, MMP-2, MMP-9, and TIMP-1 in CCSCs after treatment with Nanog or control siRNA for 48 h. Data represent the means ± SD of three independent experiments. *P < 0.05 and **P < 0.01, compared with mock; ##P < 0.01, compared with negative siRNA control.

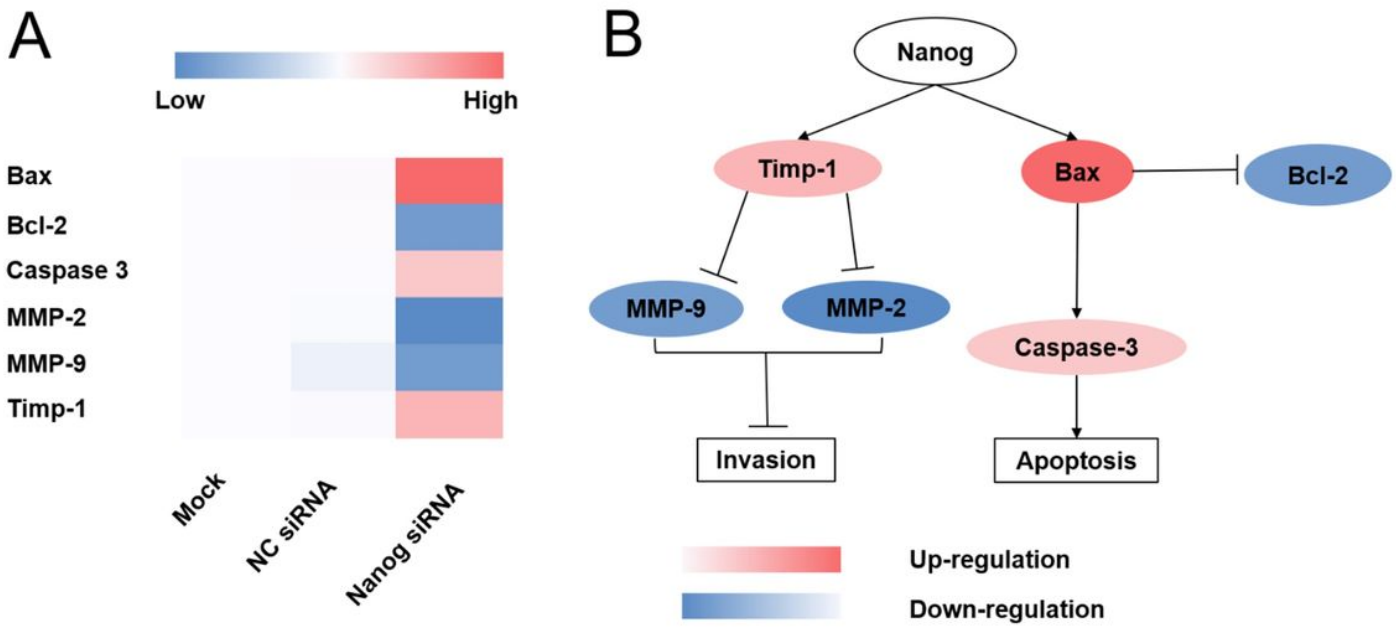

Figure 5

(A) Heat map of relative gene expression with Nanog siRNA treatment. (B) Mechanistic diagram of the effects of Nanog silencing in HCT-116 cells. Bax: Bcl-2 associated X protein; Bcl-2, B cell lymphoma-2; MMP-2, matrix metalloproteinase-2; MMP-9, matrix metalloproteinase-9; TIMP-1, tissue inhibitor of metalloproteinase-1.

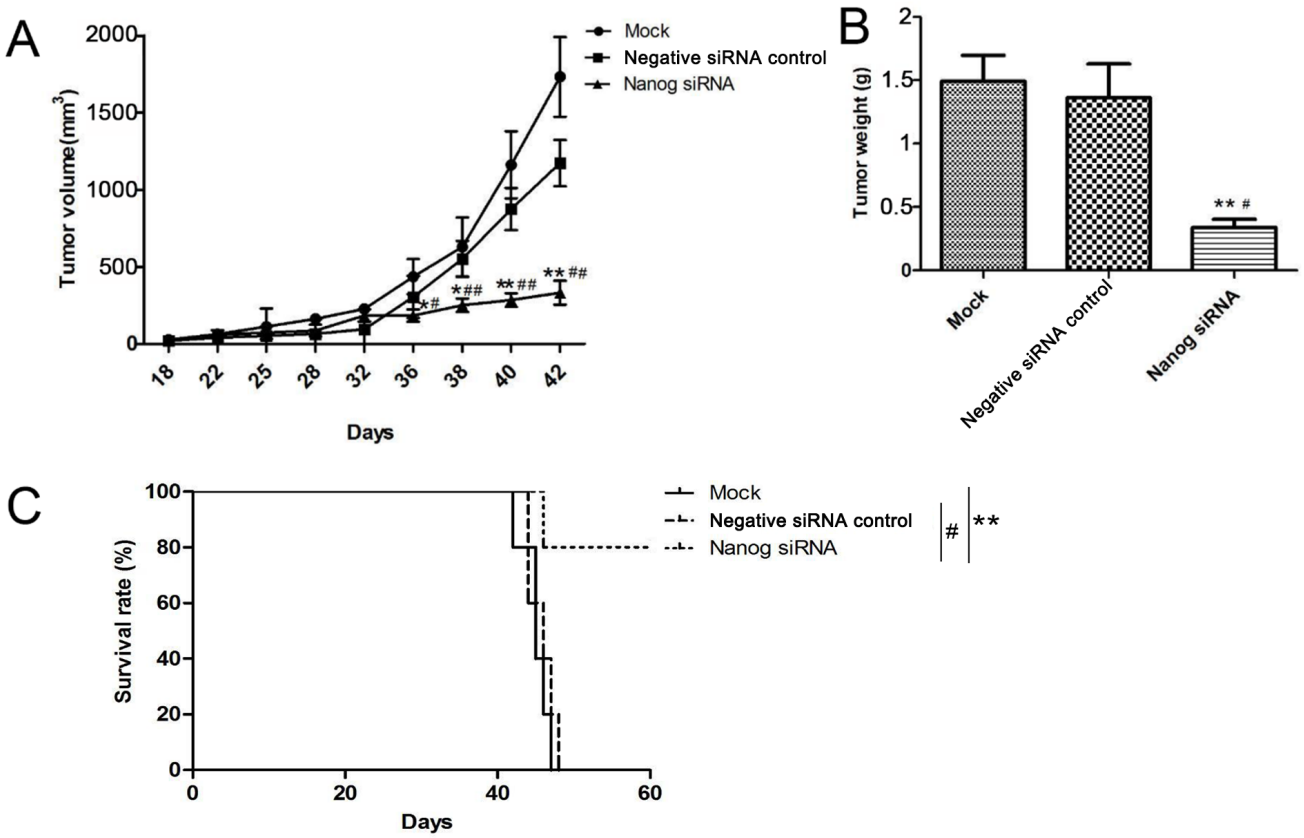

Figure 6

Nanog siRNA treatment suppressed xenograft tumor growth and prolonged mice survival. (A) Tumor volume and (B) tumor weight in the CCSCs xenograft mice following Nanog or negative siRNA control treatments for three weeks. (C) GraphPad prism 5 showing CCSCs xenograft mice survival after Nanog siRNA treatment. Data represent the means ± SD. *P< 0.05 and **P < 0.01, compared with mock; #P<0.05 and ##P<0.01 compared with negative siRNA control.